Journal of Pharmaceutical and Biomedical Analysis 121 (2016) 161–173

Contents lists available at ScienceDirect

Journal of Pharmaceutical and Biomedical Analysis

journal homepage: www.elsevier.com/locate/jpba

Practical method development for the separation of monoclonal antibodies and antibody-drug-conjugate species in hydrophobic interaction chromatoraphy, part 2: Optimization of the phase system

Alessandra Cusumano[a], Davy Guillarme[b], Alain Beck[c,1], Szabolcs Fekete[b,*]

[a] Department of Pharmacy and Biotechnology, Alma Mater Studiorum, University of Bologna, Via S. Donato 19/2, 40127, Bologna, Italy
[b] School of Pharmaceutical Sciences, University of Geneva, University of Lausanne, Boulevard d'Yvoy 20, 1211 Geneva 4, Switzerland
[c] Center of Immunology Pierre Fabre, 5 Avenue Napoléon III, BP 60497, 74160 Saint-Julien-en-Genevois, France

ARTICLE INFO

Article history:
Received 25 November 2015
Received in revised form 13 January 2016
Accepted 14 January 2016
Available online 16 January 2016

Keywords:
Hydrophobic interaction chromatography
Monoclonal antibody
Antibody-drug-conjugate
Method development
Brentuximab-vedotin

ABSTRACT

The goal of this second part was (i) to evaluate the performance of commercially available HIC columns and (ii) to develop a fast and automated "phase system" (i.e. stationary phase and salt type) optimization procedure for the analytical characterization of protein biopharmaceuticals. For this purpose, various therapeutic mAbs (denosumab, palivizumab, pertuzumab, rituximab and bevacizumab) and a cysteine linked ADC (brentuximab-vedotin) were selected as model substances. Several HIC column chemistries (butyl, ether and alkylamide) from different providers were evaluated in four different buffer systems (sodium acetate, sodium chloride, ammonium acetate and ammonium sulfate). As stationary phases, the historical TSK gel Butyl NPR phase and the brand new Thermo MAbPac HIC-10 were found to be the most versatile ones in terms of hydrophobicity, peak capacity and achievable selectivity. As salt types, ammonium sulfate and sodium acetate were found to be particularly well adapted for the analytical characterization of mAbs and ADCs, but it is important to keep in mind that a concentration 2 to 3-times higher of sodium acetate versus ammonium sulfate is required to achieve a similar retention in HIC. After selection of the most appropriate phase systems, the optimization of the separation can be carried out by computer assisted retention modeling in a high throughput manner.

1. Introduction

Hydrophobic interaction chromatography (HIC) is a reference technique to separate proteins on the basis of their hydrophobicity under native conditions [1,2]. The separation concept of HIC is based on the protein salting-out principle explained in details in the first part of this study [3].

Practical method development in HIC is rarely discussed in literature. In the first part of this work, a systematic study was presented on the optimization of gradient program, mobile phase pH, salt concentration and organic modifiers for the separation of monoclonal antibodies (mAbs) and antibody-drug conjugate (ADC) species [3]. Here, we focus on the selection of stationary phase and salt type. The combination of these two parameters is often referred to as "phase system" of HIC separations [4–6].

In the past 10–20 years, the number of commercially available analytical scale HIC stationary phases was quite limited, but this number has recently grown, thanks to the recent developments in column technology and strong interest for protein biopharmaceuticals. Standard (4.6 mm i.d.) and narrow bore (2.0–2.1 mm i.d.) columns packed with 2.5, 3, 5, 7 or 10 μm particles are available in various lengths. In addition, several chemistries including butyl, ether, phenyl, amide, amide/ethyl groups can be used for tuning retention (hydrophobicity) and selectivity [7]. Analytical scale HIC columns are based either on silica or polymeric particles, and both porous and non-porous particles are available. Highly cross-linked non-porous poly(styrene–divinylbenzene) (PS/DVB) and polymethacrylate-based particles are often used in protein separations due to their advantageous mass transfer properties, since the main contribution to the band broadening of large biomolecules, namely trans-particle mass transfer resistance is negligible. These materials can withstand pressure drop up to 100–400 bar. One of the most popular HIC column for mAbs and ADCs analysis in the pharmaceutical industry is the 35 × 4.6 mm, 2.5 μm TSKgel Butyl-NPR from Tosoh [8–12]. This is quite surprising since this material

* Corresponding author. Fax: +41 22 379 68 08.
E-mail address: szabolcs.fekete@unige.ch (S. Fekete).
[1] www.cipf.com.

http://dx.doi.org/10.1016/j.jpba.2016.01.037
0731-7085/

is available from the 90s and there are a significant number of alternative columns that have been commercialized since then. It is however worth mentioning here that there is a lack of 150 × 2.1 mm HIC column format, which is often applied for the analysis of proteins in modern chromatographic practice.

The functional groups on HIC phases are more sparsely distributed than in RP, producing moderately hydrophobic surfaces and resulting in mild interactions [4]. Retention in HIC mostly depends on the ligand type, ligand chain length and ligand density. Szepesy and Rippel showed that salt type can have different effects on retention depending on the hydrophobicity of the protein to be separated, and emphasized the importance of a well selected phase system [4]. This work also illustrated that working in HIC with gradient elution is more appropriate than isocratic elution conditions [4,13,14].

Today, the selection of phase system and operating conditions are mostly based on subjective and historical references, while the optimization is mostly carried out by trial-and-error approach. As an example, in most of the HIC applications, the above mentioned TSKgel Butyl-NPR column is almost exclusively operated in ammonium sulfate buffer. However, all the salts having salting out properties (and appropriate solubility) can be considered as potential buffer components for HIC separations. A systematic study showed the possibility to combine different salts (binary and ternary salt systems) to modify selectivity and retention in HIC [15]. In this phase system optimization concept, the experimental design was based on gradient experiments performed on three different columns and with three different buffers (salts).

In the present work, the purpose was to suggest a fast and automated phase system optimization procedure for the HIC separation of mAbs and ADCs species. In addition, the most recent stationary phases were compared to each other including the historical reference column (TSKgel Butyl-NPR). Four different salt systems were evaluated and after selection of the most appropriate phase system, the optimizations were carried out by computer assisted retention modeling. Real life samples such as denosumab, palivizumab, pertuzumab, rituximab and bevacizumab and a cysteine linked ADC (brentuximab-vedotin), all approved by the Food and Drug Administration (FDA) and the European Medicine Agency (EMA) are presented here as case studies.

2. Experimental

2.1. Chemicals and columns

Water was obtained with a Milli-Q Purification System from Millipore (Bedford, MA, USA). Sodium dihydrogen phosphate, Disodium hydrogen phosphate, ammonium sulfate, ammonium acetate and sodium chloride were purchased from Sigma–Aldrich (St. Louis, MO, USA). Sodium acetate was purchased from Fluka Chemie (Buchs, Switzerland). 1 M sodium hydroxide (NaOH) solution was purchased from VWR International S.A.S. (Fontenay-sous-Bois, France).

FDA and EMA approved therapeutic IgG monoclonal antibodies including bevacizumab (Roche, Germany), rituximab (Roche, Germany), palivizumab (Abbot, USA), denosumab (Amgen, USA) and pertuzumab (Roche, Germany) and ADC brentuximab vedotin (Seattle Genetics, USA).

MAbPac HIC-10 100 × 4.6 mm, 5 μm (1000 Å), MAbPac HIC-20 100 × 4.6 mm, 5 μm (1000 Å) and MAbPac HIC-Butyl 100 × 4.6 mm, 5 μm columns were purchased from Thermo Fisher Scientific Inc (Sunnyvale, CA, United States). Protein-Pak Hi Res HIC 100 × 4.6 mm, 2.5 μm column was a generous gift from Waters (Milford, MA, USA). TSKgel Butyl-NPR 35 × 4.6 mm, 2.5 μm column and TSKgel Ether-5PW 75 × 2.0 mm, 10 μm column were purchased from Tosoh Bioscience GMBH (Stuttgart, Germany).

2.2. Equipment and software

All the experiments were performed using a Waters Acquity UPLC™ system equipped with a binary solvent delivery pump, an autosampler and fluorescence detector (FL). The Waters Acquity system included a 5 μL sample loop and a 2 μL FL flow-cell. The loop is directly connected to the injection switching valve (no needle seat capillary). The connection tube between the injector and column inlet was 0.13 mm I.D. and 250 mm long (passive preheating included), and the capillary located between the column and detector was 0.10 mm I.D. and 150 mm long. The overall extra-column volume (V_{ext}) is about 14 μL as measured from the injection seat of the auto-sampler to the detector cell. The measured dwell volume is around 100 μL. Data acquisition and instrument control was performed by Empower Pro 3 Software (Waters). Calculation and data transferring was achieved by using DryLab 2010 (Molnar Institute, Berlin) and Excel templates (MS Office).

The mobile phase pH was measured using a SevenMulti S40 pH meter (Mettler Toledo, Greifensee, Switzerland).

2.3. Apparatus and methodology

2.3.1. Mobile phase composition and sample preparation

Generally, for the separation of mAbs and ADCs, the mobile phase "A" consisted of 1.5–4.1 M aqueous salt solution (namely 1.5 M ammonium sulfate, 3 M sodium acetate, 3.7 M sodium chloride and 4.1 M ammonium acetate) also containing 0.1 M phosphate buffer, while mobile phase "B" was 0.1 M phosphate buffer. The mobile phase pH was set by adjusting the ratio of sodium dihydrogen phosphate and disodium hydrogen phosphate and further adjusted by adding 1 M NaOH solution. The pH was set at 7.0. The salt concentration was selected on the basis of Hofmeister lyotropic series of salts.

The mAb samples were diluted in water to 2 mg/mL and ADC sample was diluted in water to 2.5 mg/mL and both stored at 4 °C in refrigerator. Then, the samples were directly injected using low volume insert vials.

2.3.2. Selection of stationary phase, flow rate and gradient time

Preliminary measurements were carried out on seven different columns. Among these columns, one was clearly not acceptable for mAb and ADC separations (because of the distorted peak shape and too high hydrophobicity). Therefore, only six columns were finally characterized. Table 1 shows some important features of the selected columns.

Generic linear gradients, starting from 0% to 100% B were applied at a constant linear velocity, corresponding to 1 mL/min and 0.21 mL/min flow rate on 4.6 mm and 2 mm ID columns, respectively. The gradient time (t_G) was varied depending on the columns length: 10 and 30 min for 4.6 × 100 mm columns, 3.5 and 10.5 min for 4.6 × 35 mm columns and 6.5 and 22.5 min for 2.0 × 75 mm columns, in agreement with the rules of geometrical method transfer [16].

2.3.3. Calculations

In gradient elution mode, the observed apparent retention factor (k_{app}) is often used to compare the retention of various compounds on different columns independently on column dimensions:

$$k_{app} = \frac{(t_r - t_0)}{t_0} \quad (1)$$

where t_r is the retention time (in gradient elution mode) and t_0 is the column dead time.

Table 1
Some important physical and chemical properties of HIC columns applied in this study.

Column name	Chemistry	Base material	Morphology	Particle size (μm)	pH	Pressure (bar)	Dimension (mm)
TSK gel Butyl-NPR	Butyl	Polymethacrylate	Non-porous	2.5	2–12	200	35 × 4.6
TSK gel Ether-5PW	Ether	Polymethacrylate	Porous	10	2–12	50	75 × 2.0
Protein-Pak Hi Res HIC	Butyl	Polymethacrylate	Non-porous	2.5	2–12	200	100 × 4.6
MAbPac HIC-Butyl	Butyl	Polymeric[a]	Non-porous	5	2–12	300	100 × 4.6
MAbPac HIC-10	Alkylamide	Silica	Porous	5	2–8	400	100 × 4.6
MAbPac HIC-20	Alkylamide	Silica	Porous	5	2–9	400	100 × 4.6

[a] No specification is available.

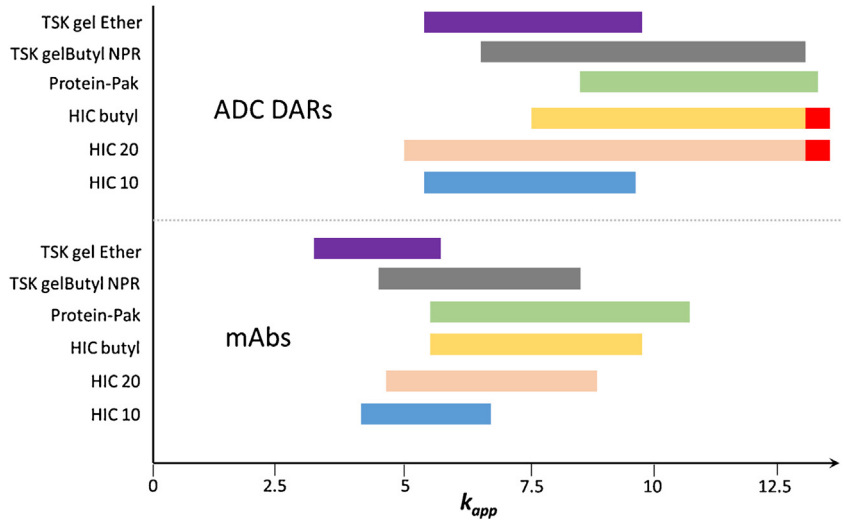

Fig. 1. Comparison of elution windows (k_{app}) obtained on different columns by using ammonium sulfate buffer (1.5 M) and running the short gradient (t_{G1}).

The linear velocity (u_0) and the total column porosity (ε_T) were determined using the following equation:

$$u_0 = \frac{L}{t_0} = \frac{4F}{\varepsilon_T d_c^2 \pi} \quad (2)$$

where L is the column length, F is the mobile-phase flow-rate and d_c is the column diameter.

The LSS model for isocratic HIC separations can be written as:

$$\log k = \log k_0 + S \times c \quad (3)$$

where k is the retention factor in isocratic elution mode, k_0 corresponds to the retention factor observed in mobile phase containing no salt, c is the salt concentration and S is the gradient steepness.

According to the LSS theory, the retention time (t_r) of a solute can be calculated in HIC conditions for any gradient using the following equation:

$$t_r = \frac{t_G}{S \times \Delta c} \log\left(\frac{2.303 \times S \times \Delta c \times t_0 \times k_0}{t_G} + 1\right) + t_0 + t_d \quad (4)$$

where t_G is the gradient time (duration) and t_d is the system dwell time (gradient delay). Eq. (4) can be rearranged to give [17]:

$$\gamma = \frac{1}{S}\log\Gamma + \frac{1}{S}(S + k_0) + \Gamma \quad (5)$$

where $\gamma = 2.303 \times \Delta c \times t_r/t_G$ and $\Gamma = 2.303 \times \Delta c \times t_0/t_G$. After further manipulation, the next formula can be obtained [17]:

$$\gamma - \Gamma = \frac{1}{S}\log\Gamma + \frac{1}{S}\log(S \times k_0) \quad (6)$$

This expression is useful since it yields $1/S$ as the slope of the linear fit of $\gamma - \Gamma$ versus $\log\Gamma$.Finally, the $\log k_0$ and S parameters of the HIC LSS model can be determined from two linear gradient runs obtained with different t_G. For extracting the parameters, DryLab 2010 software was used.

After getting the LSS parameters, the hydrophobicity index (c^*) was calculated as [6,15,18]:

$$c* = \frac{\log k_0}{S} \quad (7)$$

where c^* corresponds to the salt concentration at which $\log k = 0$ ($k = 1$) in isocratic mode. This c^* value reflects well the properties of both the stationary phase and salt type and may be useful for characterization and comparison of the HIC phase systems.

In gradient elution mode, peak capacities were experimentally determined from the gradient time and the average measured peak width at 50% height ($W_{50\%}$). The following equation was used to estimate the peak capacity based on peak width at 4σ, corresponding to a resolution of $R_s = 1$ between consecutive peaks:

$$P = 1 + \frac{t_G}{1.7 \times w_{50\%}} \quad (8)$$

To avoid the imprecision associated with the measurement of peak widths at baseline for proteins often containing closely related variants (i.e. for a heterogeneous sample), the peak width at half height was preferred in this study. This way, the impurities present in the sample, and partially resolved from the main component, did not confuse the measurement.

2.3.4. Investigation of retention properties of mAbs and ADC DARs (brentuximab vedotin)

Intact mAbs and ADCs species were eluted in linear inverse salt gradient mode. For studying the retention properties of intact mAbs, five model therapeutic antibodies were selected based on their type (IgG class and isotype), calculated isoelectric point (p*I*) and hydrophobicity. The purpose was to cover the common p*I* range of mAbs and to include chimeric (ch), humanized (hz) and human (hu) reference IgG1 and IgG2 isotypes, to draw overall and reliable conclusions. The selected mAbs were the following in the

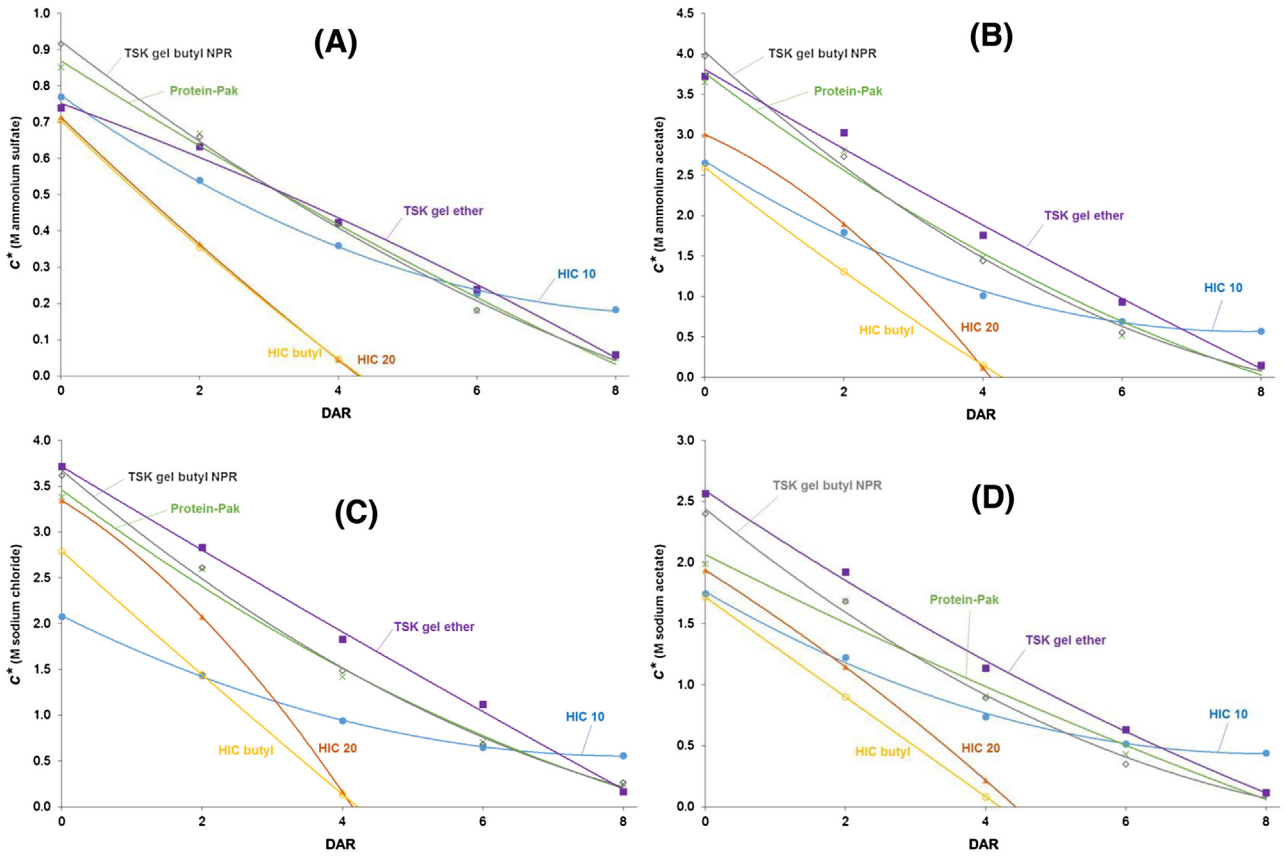

Fig. 2. Plots of hydrophobicity indexes (c^*) of ADC species (brentuximab vedotin) versus DAR numbers, obtained on the different columns and salts: ammonium sulfate (A), ammonium acetate (B), sodium chloride (C) and sodium acetate (D).

order of their hydrophobicity (HIC elution order based on preliminary study): denosumab (huIgG2, p*I* = 8.8), palivizumab (hzIgG1, p*I* = 9.0), pertuzumab (hzIgG1, p*I* = 8.7), rituximab (chIgG1, p*I* = 9.1) and bevacizumab (hzIgG1, p*I* = 8.5).

For studying the retention properties of the different populations of ADC molecules that differ in the number of drugs per antibody, which are often known as DARs (drug-to-antibody ratios) species [19,20], the cysteine linked IgG1 type brentuximab vedotin was selected as it is the first approved cysteine linked ADC available on the market. Brentuximab vedotin is a chIgG1 class antibody including peptide linker and auristatin E as cytotoxic drug [21,22]. This ADC can possess DAR0, DAR2, DAR4, DAR6 and DAR8 species, from which DAR0 is the naked mAb, while DAR2, DAR4, DAR6 and DAR8 contains 2, 4, 6 and 8 drugs on the mAb, respectively. The different species can also include different positional isomers.

First, the different phase systems were evaluated by means of two gradient runs (gradient steepness was different by a factor of 3) performed on the six different columns and with four different salt systems. Generic linear gradients, starting from 0 to 100% B were applied under the conditions specified in section 2.3.2.

For the comparison of the different phase systems, the elution window of the mAbs and DAR species of ADC were plotted versus the apparent retention factor. This way, the elution windows and the hydrophobicity of the different phase systems can be compared in a practical way.

Then – based on the two gradient runs – the parameters of the LSS models were derived and the hydrophobicity indexes for each solute and phase systems were determined and compared. The hydrophobicity of some phase systems was found to be critical for the most hydrophobic DAR species. For better understanding this phenomena, plots of c^* values versus DAR numbers were prepared. This way, the appropriate phase systems could be selected for the DAR species separations.

For the separation of DAR species, it seemed that very similar retention and selectivity can be attained with all of the appropriate phase systems. Therefore c^* values obtained with different salt systems (i.e. ammonium acetate, sodium chloride and sodium acetate) were plotted as a function of c^* observed with the reference ammonium sulfate buffer system. Then, the equivalent salt concentration – providing the same retention and selectivity for DAR species – of different salt systems could be determined. Peak capacities obtained with the different phase systems were also compared.

2.3.5. Systematic method optimization

A general approach for multidimensional experimental design consists in simultaneously modeling the effect of the most important factors i.e. gradient steepness and temperature or pH on selectivity on a previously selected column [23,24]. Then, with the help of resolution maps generated by modeling software – showing the critical resolution of the peaks to be separated [27] – the selected variables can be rapidly and efficiently optimized. This approach was currently applied for the RP, IEX and HIC separation of antibody variants [3,25,26,27].

For the optimization of mAb separations, experimental designs with 4 runs were performed. Performing gradient runs with two different gradient times (as $t_{G1} = 10$ min, $t_{G2} = 30$ min on 100×4.6 mm columns) and two mobile phase temperatures (20 and 40 °C) allowed a reliable optimization. The latter was performed by computer modeling using DryLab software. A mixture of reference mAbs was injected to build up the retention models.

On the other hand, for separating the DAR species of ADC, only the gradient steepness was found to be an important variable for

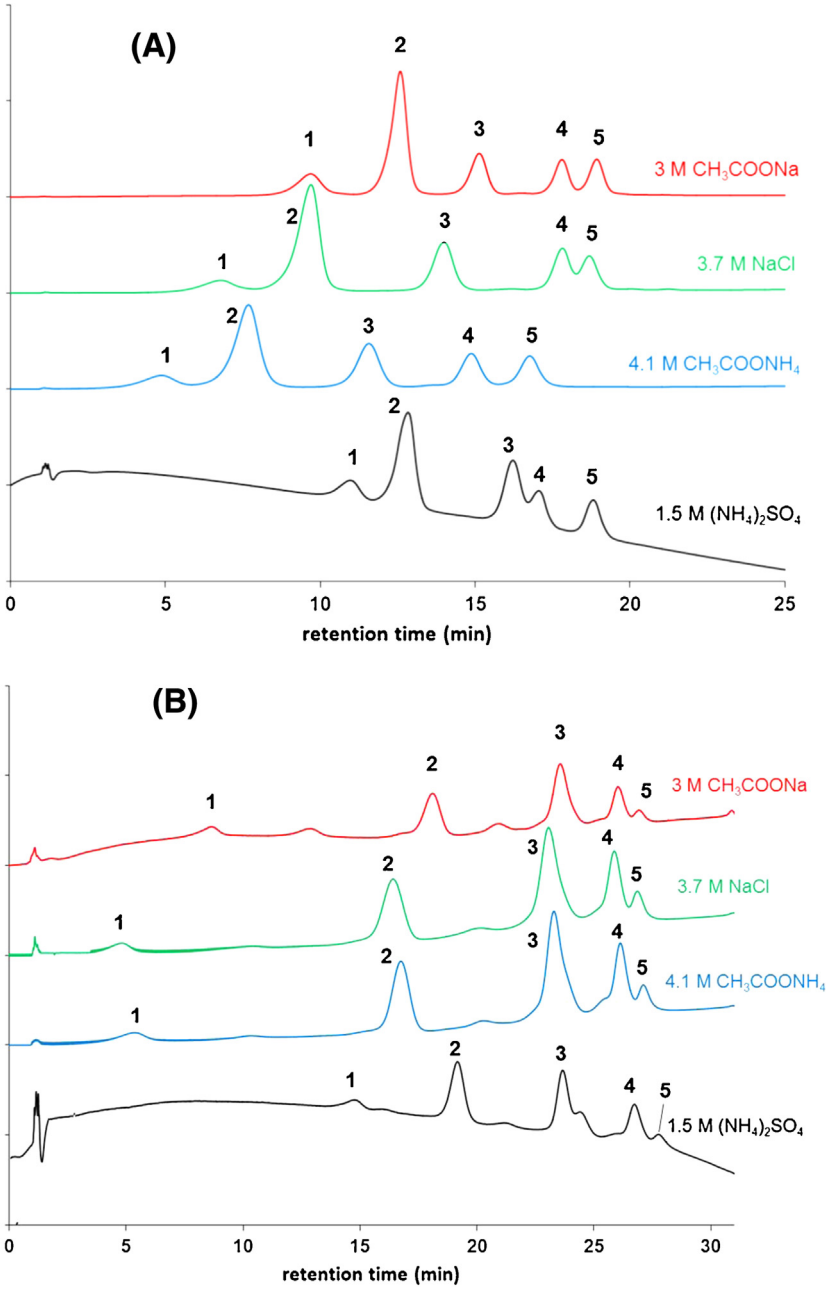

Fig. 3. Representative chromatograms obtained on MabPac HIC 10 (100 × 4.6 mm, 5 μm) column by using different salt systems. Flow rate: 1 mL/min, gradient: 0–100% B in 30 min, temperature: 20 °C, detection: fluorescence (λ_{ex}: 280 nm, λ_{em}: 360 nm), sample: mAb mixture (A) and commercial ADC (B).

method optimization [3]. So finally, performing two initial gradients with gradient times of t_{G1} = 10 min and t_{G2} = 30 min at T = 20 °C allowed the optimization of DARs separation. Again, optimization was supported by computer modeling. The accuracy of retention time prediction was also evaluated.

3. Results and discussion

3.1. Evaluation and comparison of retention in different phase systems

Stationary phases applied for HIC separations are similar to those used in RPLC, except that the bonding is less dense and the bonded ligands are less hydrophobic (e.g., ether or butyl) due to shorter alkyl chains [24]. The combination of a less hydrophobic packing with purely aqueous mobile phases minimizes protein denaturation and usually allows the recovery of native (non denatured) proteins from separated fractions, especially for separations carried out at ambient temperature.

Retention and selectivity in HIC can be tuned by means of several operating parameters, such as stationary phase hydrophobicity, salt lyotropic strength, gradient program, temperature, organic modifier. The influence of various parameters on HIC separations of mAbs and ADC species, including gradient steepness, pH, ionic strength and organic modifiers, has been evaluated in the first part of this study. Here, our purpose was to evaluate and compare several phase systems for mAb and ADCs analysis.

Some recent butyl, ether and alkylamide (as well as a reference butyl) phases were evaluated in four different buffer systems. Table 1 summarizes some important features of the applied station-

Table 2
List of hydrophobicity indexes (c^*) for various HIC phase systems, for different mAbs and DAR species of ADC.

MAbPac HIC 10	$(NH_4)_2SO_4$	CH_3COONH_4	NaCl	CH_3COONa
mAb 1	0.95	3.29	2.77	2.04
mAb 2	0.87	2.96	2.48	1.79
mAb 3	0.68	2.38	1.93	1.50
mAb 4	0.67	1.89	1.40	1.21
mAb 5	0.55	1.68	1.40	1.12
DAR 0	0.77	2.65	2.08	1.75
DAR 2	0.57	1.80	1.44	1.22
DAR 4	0.36	1.01	0.94	0.74
DAR 6	0.23	0.69	0.65	0.52
DAR 8	0.18	0.57	0.56	0.44
MAbPac HIC 20	$(NH_4)_2SO_4$	CH_3COONH_4	NaCl	CH_3COONa
mAb 1	0.84	3.35	3.10	1.95
mAb 2	0.70	2.43	2.48	1.50
mAb 3	0.69	1.97	1.80	1.49
mAb 4	0.44	0.88	1.11	1.08
mAb 5	0.09	0.22	0.28	0.16
DAR 0	0.71	3.00	3.35	1.94
DAR 2	0.36	1.90	2.08	1.15
DAR 4	0.04	0.12	0.16	0.22
DAR 6	n.e.	n.e.	n.e.	n.e.
DAR 8	n.e.	n.e.	n.e.	n.e.
MAbPac HIC Butyl	$(NH_4)_2SO_4$	CH_3COONH_4	NaCl	CH_3COONa
mAb 1	0.87	3.12	2.91	1.84
mAb 2	0.75	2.64	2.32	1.47
mAb 3	0.56	1.93	1.66	1.16
mAb 4	0.44	1.21	0.90	0.80
mAb 5	0.30	0.90	0.78	0.63
DAR 0	0.71	2.60	2.79	1.72
DAR 2	0.36	1.31	1.44	0.90
DAR 4	0.05	0.15	0.14	0.08
DAR 6	n.e.	n.e.	n.e.	n.e.
DAR 8	n.e.	n.e.	n.e.	n.e.
Protein-Pak HiRes	$(NH_4)_2SO_4$	CH_3COONH_4	NaCl	CH_3COONa
mAb 1	1.10	4.10	4.15	2.18
mAb 2	1.02	3.66	3.28	2.17
mAb 3	0.87	2.86	2.73	1.95
mAb 4	0.76	2.39	1.95	1.58
mAb 5	0.65	1.55	1.68	1.37
DAR 0	0.85	3.65	3.38	1.99
DAR 2	0.67	2.81	2.60	1.69
DAR 4	0.42	1.48	1.42	0.90
DAR 6	0.18	0.51	0.71	0.43
DAR 8	0.05	0.13	0.25	0.11
TSK gel butyl NPR	$(NH_4)_2SO_4$	CH_3COONH_4	NaCl	CH_3COONa
mAb 1	1.09	4.01	3.28	2.21
mAb 2	1.01	3.54	2.84	2.16
mAb 3	0.86	2.71	1.88	1.94
mAb 4	0.74	2.25	1.75	1.51
mAb 5	0.62	1.41	1.66	1.31
DAR 0	0.92	3.97	3.62	2.40
DAR 2	0.66	2.73	2.61	1.68
DAR 4	0.42	1.44	1.49	0.89
DAR 6	0.18	0.56	0.68	0.35
DAR 8	0.05	0.12	0.26	0.10
TSK gel ether	$(NH_4)_2SO_4$	CH_3COONH_4	NaCl	CH_3COONa
mAb 1	1.18	5.05	4.60	3.65
mAb 2	1.06	5.05	3.88	3.52
mAb 3	0.93	4.57	3.45	2.48
mAb 4	0.84	3.46	2.46	1.96
mAb 5	0.64	2.68	2.14	1.49
DAR 0	0.74	3.73	3.71	2.56
DAR 2	0.63	3.03	2.83	1.92
DAR 4	0.42	1.76	1.83	1.14
DAR 6	0.24	0.93	1.12	0.63
DAR 8	0.06	0.15	0.17	0.12

n.e.: not eluted.

ary phases, while Fig. 1 shows a comparison of elution windows obtained with the reference ammonium sulfate buffer (1.5 M) on all stationary phases (observed with the shortest gradient (t_{G1})) for the ADC species (DAR0, DAR2, DAR4, DAR6 and DAR8) and also for the mixture of 5 model mAbs. Apparent retention factors are shown, to have a comparison independent on column dimensions. Similar conclusions can be drawn when applying other salt systems (data not shown). As can be seen, the widths of the gradient windows and the k_{app} values were quite different on the six columns. For the mixture of mAbs, the HIC 10 and the TSK-gel ether columns resulted in the lowest retention, while the Protein-Pak provided the highest retention and largest elution window. Overall, all the columns showed appropriate hydrophobicity for the analysis of mAbs. Please note that the selected mAbs cover the whole hydrophobicity range of commercially available IgG-s and antibodies under development.

In comparison with mAbs, the ranking of columns shows huge differences when characterizing DARs species of ADC. The DAR species of brentuximab vedotin cover a significantly broader hydrophobicity range than the naked mAbs. Species with 6 or 8 linked cytotoxic drugs are indeed very hydrophobic and they are not able to elute from the HIC 20 and HIC butyl columns, even without salt in the mobile phase (100% B eluent). Therefore, these two columns are not acceptable for ADC characterization, in terms of hydrophobicity. The four other columns enabled the elution of all DAR species in all salt systems, confirming that they are appropriate for the analysis of cysteine linked IgG1 type ADCs, at least in terms of hydrophobicity.

The hydrophobicity indexes (c^*) were derived for all solutes and all conditions. Table 2 shows the corresponding c^* values. Since hydrophobic interactions mostly depend on the size of hydrophobic surfaces of the solute, an obvious trend is expected for ADC, when plotting c^* values versus the DAR numbers. Fig. 2 shows these plots for all tested conditions (salts and columns). In ammonium sulfate buffer, (Fig. 2(A)), five columns show more or less linear behavior, expect HIC 10 that provides a slight convex curvature. Moreover the HIC 10 column shows somewhat unique behavior whatever the salt in the mobile phase is. In ammonium acetate, sodium chloride and sodium acetate (Fig. 2(B–D)), the curve of HIC 20 shows a concave behavior. The TSK gel butyl NPR, TSK gel ether and Protein-Pak columns show very similar behavior (trend and slope) in each salt system. The plots also confirm that HIC 20 and HIC butyl columns are inadequate for the elution of high DARs. Indeed, the curves corresponding to these two columns cross the x axis just after the DAR4, proving that DAR6 and DAR8 species cannot be eluted from these columns whatever the mobile phase composition. Finally, these representations illustrate that the hydrophobicity of DAR species is directly proportional to the number of linked drugs and suggest that retention of ADC species in HIC is mostly driven by the number of linked drugs.

For mAbs, the hydrophobicity indexes vary significantly within the different phase systems, but the elution order remains identical in each condition. Their c^* values were quite different depending on the columns, for the same salt system. This suggests that retention and selectivity strongly depend on the stationary phase. When having a look to the c^* values obtained on one column and different salt systems, their relative ratios ($c^*/c^*_{reference}$) also slightly change. In other words, the selectivity of mAb separations performed on one given column can also be tuned by changing the salt type.

Figs. 3 and 4 show some representative chromatograms for illustrating the hydrophobicity and selectivity of different phase systems. The chromatograms on Fig. 3 correspond to one unique column (HIC 10) and four different salt systems. On the contrary, Fig. 4 corresponds to one unique salt system (sodium acetate), but various stationary phases. Fig.3(A) illustrates that retention and

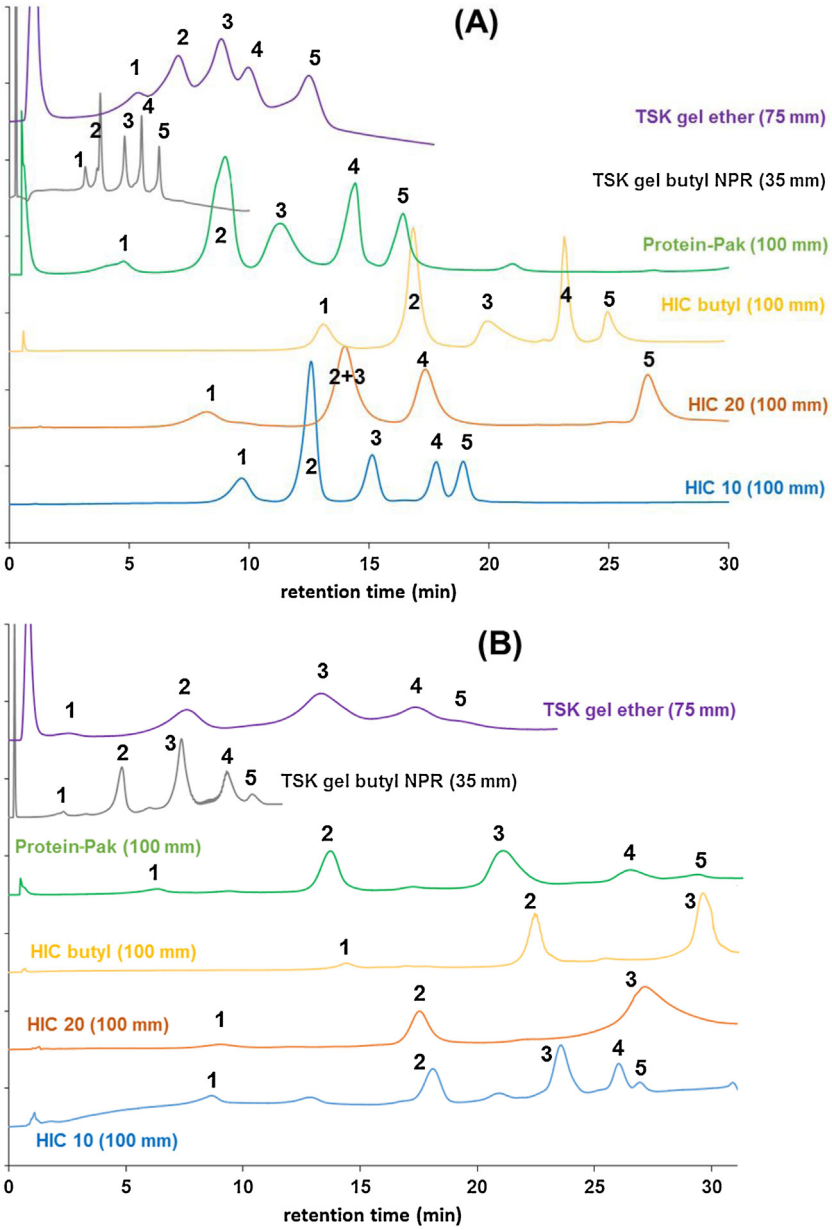

Fig. 4. Representative chromatograms obtained on different columns by using sodium acetate salt system. Flow rate: 1 mL/min on 4.6 mm i.d. columns and 0.21 mL/min on 2 mm i.d. columns, gradient: 0–100% B (applying the short gradient time: t_{G1}), temperature: 20 °C, detection: fluorescence (λ_{ex}: 280 nm, λ_{em}: 360 nm), sample: mAb mixture (A) and commercial ADC (B).

selectivity of mAbs in HIC can be tuned by changing the salt system. Fig. 3(B) suggests – at first sight – that when the lyotropic strength of the different salts is corrected (equivalent in the initial mobile phase composition), more or less the same selectivity can be achieved for ADC species (the retention times of peaks 3, 4 and 5 are identical, only peaks 1 and 2 show deviances) More explanations for this observation are provided in section 3.3.

Fig. 4(A) is a good example illustrating the importance of the stationary phase chemistry in HIC. Very different selectivities (but no elution order modification) can be attained with one given salt system on different stationary phases – at least for mAb separations. Fig. 4(B) shows that an appropriate selectivity between DAR peaks is feasible on any HIC column, but the most important feature of the column is its hydrophobicity. Indeed, some of the current commercial HIC columns are clearly too hydrophobic for ADC characterization.

3.2. Comparison of peak capacity in different phase systems

Observed peak capacities were practically the same in different salt systems on one given column, suggesting that the salt type does not alter significantly peak broadening. However, the efficiency was strongly modified between columns. This behavior was expected since the columns employed in this study possess different particle size, column length and particle morphology. For practical reasons, the peak capacity values were not extrapolated to a fixed column length, since not all the column dimensions are commercially available. As example, the peak capacity achieved on one of the most popular HIC columns with dimensions of 35 × 4.6 mm, was compared to that achieved on the 100 mm MAbPac HIC-Butyl column. Table 3 summarizes the peak capacity values obtained with ammonium sulfate buffer with the short (t_{G1}) and long (t_{G2}) gradients (the same conclusion can be drawn with the other salt systems). For mAbs and ADC species, the MabPac HIC butyl and TSK gel butyl

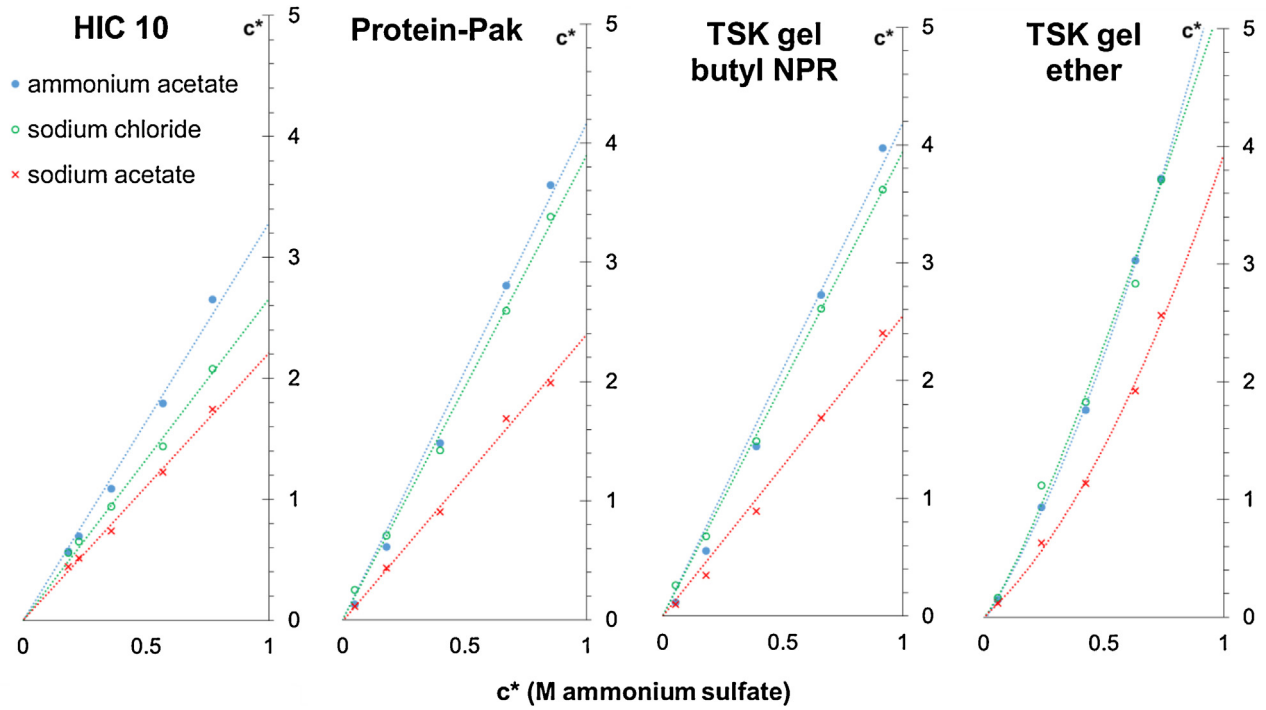

Fig. 5. Plots of c^* values observed in different salt systems versus c^* of reference salt system (ammonium sulfate) on various columns (i.e. HIC 10, Protein-Pak, TSK butyl NPR and TSK gel ether).

Table 3
Peak capacities achieved with ammonium sulfate buffer on different columns and gradient times.

	mAbs		ADC	
	$P(t_{G1})$	$P(t_{G2})$	$P(t_{G1})$	$P(t_{G2})$
HIC 10	22.1	34.6	21.2	30.2
HIC 20	24.9	30.9	20.8	29.3
HIC butyl	45.2	48.3	32.3	36.3
Protein-Pak	37.1	38.0	19.2	23.8
TSK gel butyl NPR	35.6	64.9	25.6	32.4
TSK gel ether	10.9	16.7	12.2	15.8

NPR columns provided the highest peak capacities, despite the fact that the column lengths were very different. On the other hand, the lowest efficiency was achieved on the TSK gel ether column, which is logical since this column is packed with 10 μm fully porous particles.

3.3. Attaining the same selectivity for ADC species with diferent salt systems

As illustrated in our previous work, the salt type and concentration are important variables for tuning retention and selectivity of closely related proteins (such as DARs of ADC) [3]. Similar selectivities were obtained for the different DAR species of brentuximab Vedotin, using different salts on one given column, when the lyotropic strength was corrected [3]. In this study, the results presented in section 3.2 also suggest the same behavior, but extend this finding to various stationary phases. For comparing the hydrophobicity and achievable selectivity (related to the hydrophobicity indexes in HIC), the plots of c^* observed in one salt system versus c^* of reference salt system (ammonium sulfate) was made in Fig. 5. On the HIC 10, Protein-Pak and TSK butyl NPR phases, the correlations were linear. The fitted straight lines cross the origin, and only the slopes were different. This proves that very similar retention and selectivity can be obtained with all the four salt systems, when correcting the salt concentration (tuning the slope) for the same lyotropic strength. On the TSK gel ether column, some deviations from linearity were observed particularly with sodium acetate, while the selectivity remains similar (linear behavior) with ammonium acetate and sodium chloride.

By reading the intercepts at $c^* = 1$ with ammonium sulfate (at x axis value of 1), the equivalent molarity of the other salt systems can be obtained. As example, on the HIC 10 column, 1 M ammonium sulfate is equivalent to 2.2 M sodium acetate, 2.6 M sodium chloride and 3.3 M ammonium acetate. Similarly, 2.4 M sodium acetate, 3.9 M sodium chloride and 4.2 M ammonium acetate can replace 1 M ammonium sulfate on the Protein-Pak column. The TSK gel butyl NPR column showed similar behavior to the Protein-Pak (in terms of salt interchangeability). On the TSK gel ether column, significantly higher salt concentration was required to maintain the same selectivity and retention. By using this column, the 1 M ammonium sulfate was equivalent with 3.9 M sodium acetate, and can be replaced by 5.2 M and 5.4 M sodium chloride and sodium acetate, respectively.

Please note that only four columns were used for this comparison, since the other two (HIC 20 and HIC butyl) were not appropriate to elute the hydrophobic DAR species.

All the results presented here confirm that salt type does not play an important role in selectivity when separating the DAR species of an ADC. By adjusting the salt concentration (i.e. lyotropic strength that is relative and depends on stationary phase), very similar retention and selectivity can be attained with various salt types.

3.4. Speeding up the HIC separations of mAbs by using two dimensional retention models on different stationary phases

In a recent study, column screening and comparison were performed by their resolution maps under RPLC conditions [28]. As suggested in the present work, the peak movements and changes in selectivity/resolution can be assessed; therefore the columns

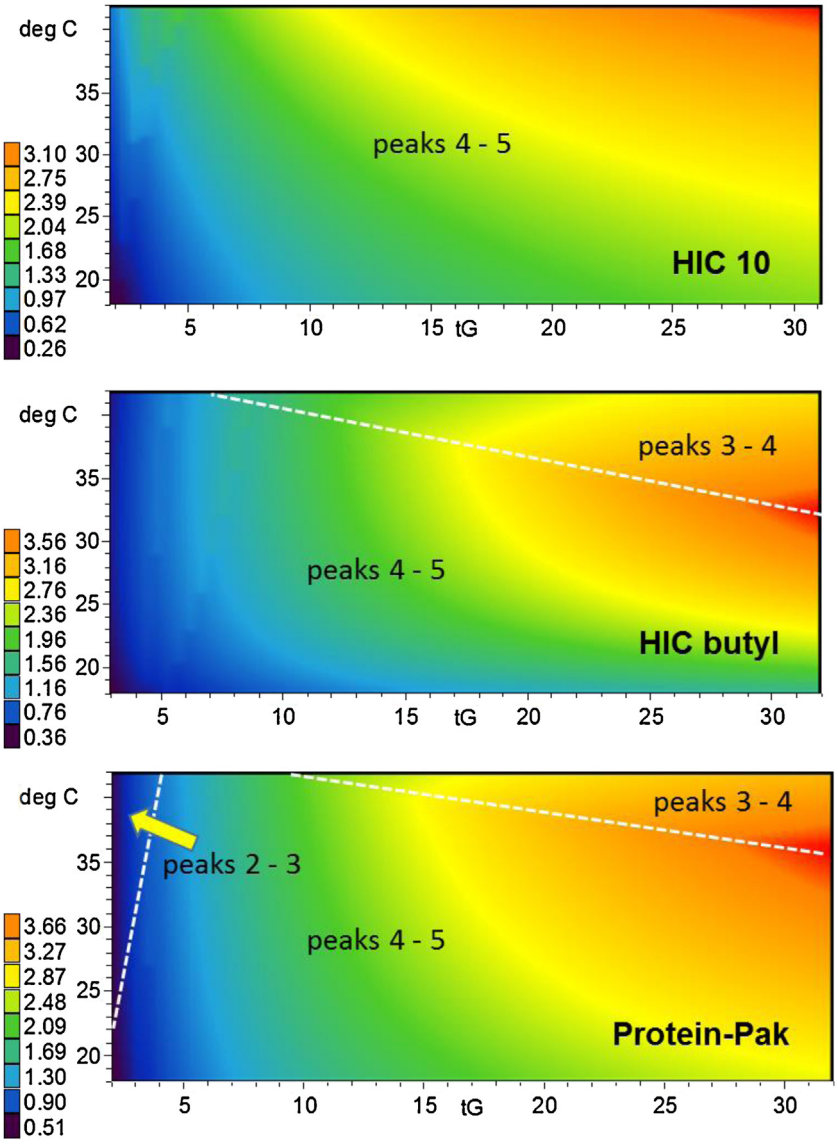

Fig. 6. Two dimensional resolution maps for mAbs mixture obtained with the HIC 10, HIC butyl and Protein-Pak columns. Variables: gradient time (t_G) and mobile phase temperature (°C). The red zones indicate high resolution conditions, while blue areas correspond to low resolution conditions (see the color codes on the figure).

can be easily ranked in terms of achievable resolution. Moreover, the differences of phase systems can also be highlighted by the comparison of resolution maps. This approach was used here for comparing HIC phase systems, and DryLab software was used to create the resolution maps. This software implements an interpretive approach, where the retention behavior is modelled using experimental information from initial runs, and the retention times at any conditions are predicted in a selected experimental domain. This allows calculating the critical resolution, and accordingly, the optimal separation conditions can be found [29,30].

As shown in our previous study, the gradient steepness has a significant impact on selectivity for mAbs separations under HIC conditions. Besides the gradient steepness, temperature can also alter the selectivity [3]. However, the mobile phase temperature should be kept within a limited range, since physiological-like conditions have to be maintained in HIC.

Two dimensional models were created with two different gradient times (10 and 30 min on 100 mm long columns) and two temperatures (T_1 = 20 and T_2 = 40 °C). Mobile phase "A" contained 3 M sodium acetate and 0.1 M phosphate buffer, while mobile phase "B" consisted of 0.1 M phosphate buffer. The pH was set to 7.0 and a flow rate of 1 mL/min was applied on these 4.6 mm i.d. columns. Please note, that sodium acetate was used in this part of the work instead of the widely used ammonium sulphate, to show its potential for HIC separations of protein biopharmaceuticals. In addition, sodium acetate gradients provide flat baseline in both UV and FL detection mode, while with ammonium sulfate gradients, a baseline drift is generally observed. The retention models were built up for the HIC 10, HIC butyl and Protein-Pak columns. Following the execution of the input experimental runs, the figures of merit (i.e. retention times, peak widths and peak tailing values) were imported into DryLab and peak tracking was performed on the basis of peak areas and individual mAbs injections. Retention times were transformed into retention factors, and linear models were chosen for the modeling retention as functions of t_G and temperature.

Fig. 6 shows the resolution maps obtained on the three different columns by using the same salt (sodium acetate) in the mobile phase. On the resolution maps, the smallest resolution (*Rs*) value of any two critical peaks in the chromatogram was plotted as a function of the two varied experimental parameters.

Based on Fig. 6, the resolution maps show some differences. First of all, the optimum resolution was achieved at a different tempera-

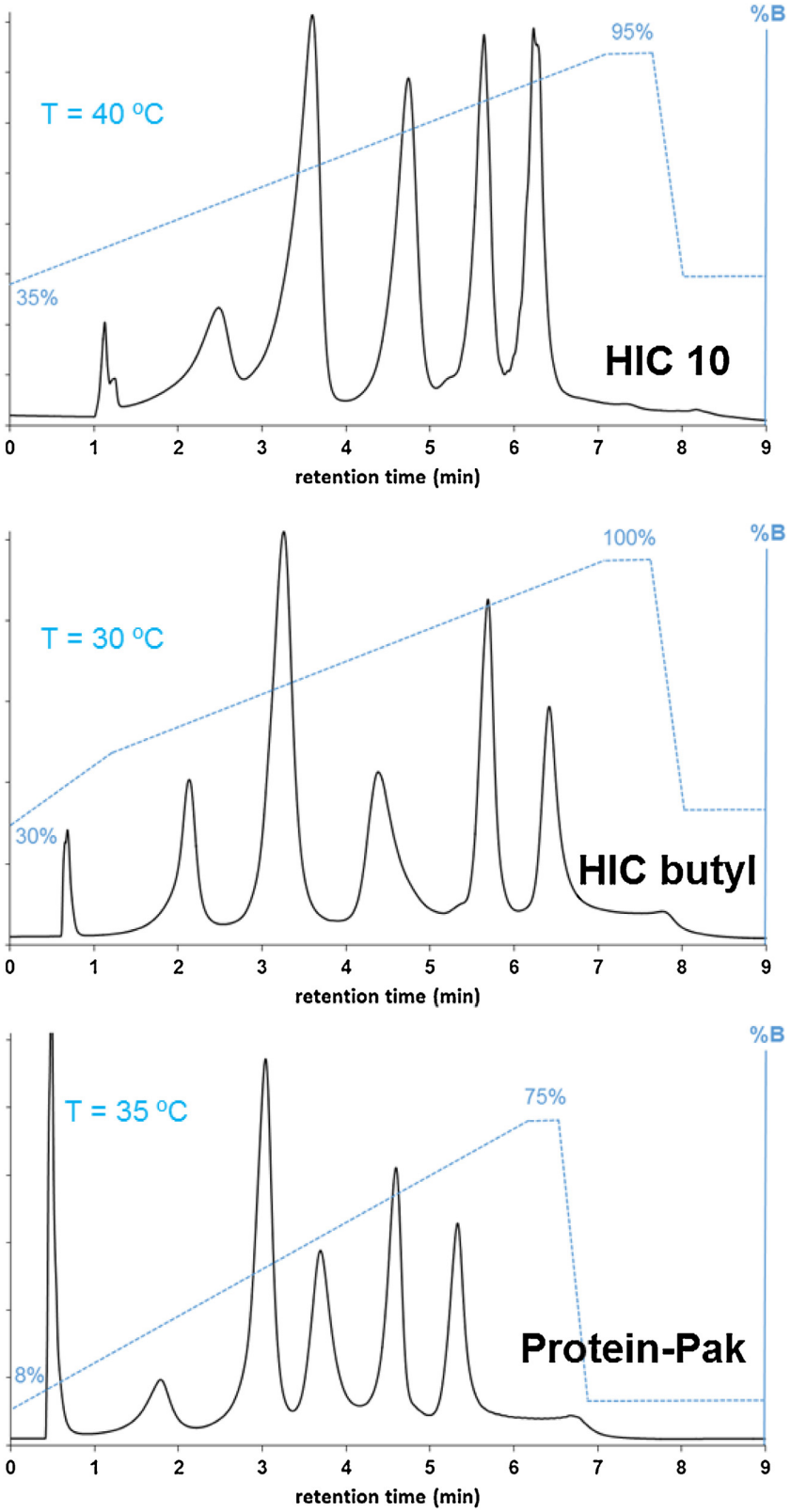

Fig. 7. Optimized mAb separations on the HIC 10, HIC butyl and Protein-Pak columns. Mobile phase, "A": 3 M sodium acetate + 0.1 M phosphate (pH 7), "B": 0.1 M phosphate (pH 7). Flow rate: 1 mL/min, gradient program and temperature are indicated on the figure. Detection: fluorescence (λ_{ex}: 280 nm, λ_{em}: 360 nm).

ture. On the HIC 10 column, the optimum occurs at above T = 40 °C, while on the HIC butyl and Protein-Pak columns, the optimum mobile phase temperature was 35 °C. The maximum resolution that can be achieved was finally quite similar on all columns (Rs_{max} between 3 and 4), and the critical peak pairs were indicated on the resolution maps. Our purpose was to speed up the separation as much as possible. For that purpose the initial and final mobile phase composition have been varied to perform equidistant reten-

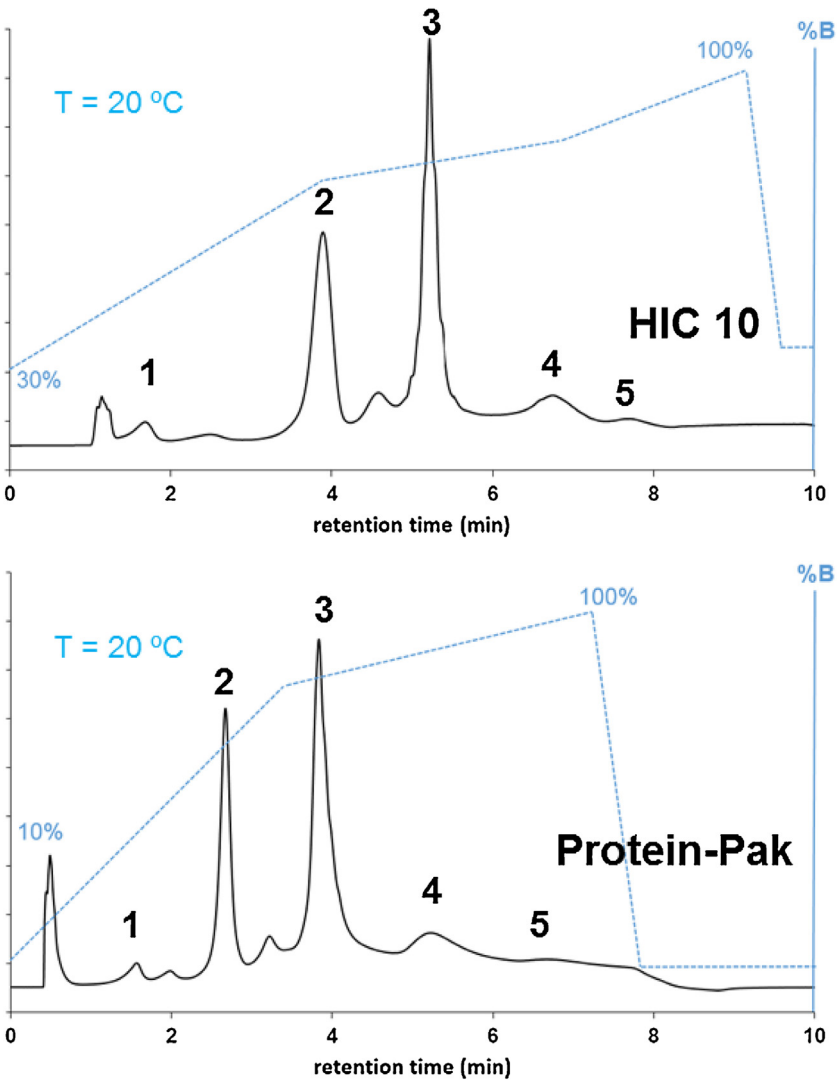

Fig. 8. Optimized ADC separations on the HIC 10 and Protein-Pak columns. Mobile phase "A": 3 M sodium acetate + 0.1 M phosphate (pH 7), "B": 0.1 M phosphate (pH 7). Flow rate: 1 mL/min, gradient program is indicated on the figure. Detection: fluorescence (λ_{ex}: 280 nm, λ_{em}: 360 nm).

tion distribution and to eliminate the "non-eluting spaces" from the chromatogram. After performing the optimization, quite similar separation quality could be achieved on the three columns. Fig. 7 shows the experimentally observed optimized separations and the corresponding conditions.

As shown, the analysis time, resolution and peak capacity were very close on the three selected columns.

To evaluate the accuracy of this approach, the predicted and experimental retention times as well as resolution values were compared. The predicted retention times were in good agreement with the experimental ones, as the average retention time relative errors were ~2.0%. The average relative errors in resolution prediction were systematically lower than 30%. (Please note that resolution prediction also takes peak width and peak shape into account).

The whole optimization procedure took only about 2 h (2 gradients with t_{G1} = 10 min and t_{G2} = 30 min × 2 temperatures at T_1 = 20 and T_2 = 40 °C × 1 sample + equilibration gives about: 10 min × 2 + 30 min × 2 + 20–30 min equilibration) on one column.

This example well illustrates that column chemistry plays an important role in HIC separations of mAbs, and also confirms that a similar separation quality can be attained on different stationary phases, by adjusting the working point of a design space (e.g. working at the optimal resolution).

3.5. Speeding up the HIC separation of DAR species of ADC, by using one dimensional retention models on different stationary phases

Based on our results for the separation of DAR species of Brentuximab Vedotin, the only relevant parameter for tuning selectivity on a selected stationary phase is the gradient steepness (gradient program) [3]. Gradient times were set to t_{G1} = 10 min and t_{G2} = 30 min, and mobile phase pH was kept constant (pH 7). Again sodium acetate was selected as the mobile phase salt (see section 3.4.).

Retention models and resolution maps were created with DryLab. Fig. 8 shows the optimized separations and the corresponding conditions. Again, our purpose was to speed up the analysis (perform the analysis below 10 min), while maintaining sufficient resolution, this is why multi-linear gradients were employed. Generally, the selectivity between DAR species is significantly larger for early eluting DAR species (DAR0, DAR2 and DAR4), while it is more critical between DAR6 and DAR8 (see Figs. 3 and 4 obtained with linear gradients). By using multi-linear gradients, the selectivity between the less hydrophobic DARs can be decreased (to eliminate the "non-eluting spaces" from chromatogram with a steeper gradient), while selectivity (and resolution) can be improved between DAR6 and DAR8 (by applying a flatter gradient segment). The final

analysis time was similar on the two columns, but the peak capacities were somewhat different. On the Protein-Pak column, $P = 32$ could be reached under the optimal conditions, while only $P = 22$ was observed with the HIC 10 column. The prediction accuracy was somewhat better than for the mAbs, which is logical since a one-dimensional retention model was employed here.

This optimization procedure took only 1 h (2 gradients × 1 sample + equilibration) per column. However, it has to be mentioned that the scouting runs for finding the appropriate salt concentrations and stationary phase may be more time consuming (depending on the number of columns used for the screening procedure).

4. Conclusion

In the present study, various phase systems were compared for HIC characterization of protein biopharmaceuticals. For this purpose, six HIC columns from different providers were tested with four different buffer systems, commonly used in HIC (i.e. sodium acetate, sodium chloride, ammonium acetate and ammonium sulfate), for the analytical characterization of therapeutic mAbs (denosumab, palivizumab, pertuzumab, rituximab and bevacizumab) and a cysteine linked ADC (brentuximab-vedotin). All the tested HIC stationary phases are bonded with moderately hydrophobic ligands (i.e. butyl, ether and alkylamide) and the bonding density is also low, to have reasonable stationary phase hydrophobicity. It appeared that two stationary phases, namely the Thermo HIC butyl and Thermo HIC 20 were adapted for mAbs analysis, but were unsuitable for the elution of the most hydrophobic DAR species (DAR6 and DAR8) of brentuximab vedotin. The four other columns were able to elute all mAbs and DAR species of ADC, but some significant differences were observed between them in terms of hydrophobicity, achievable selectivity and peak capacity. At the end, the historical TSK gel butyl NPR phase and the brand new Thermo MAbPac HIC 10 were found to be the most versatile ones for HIC of protein biopharmaceuticals. In terms of salt type, significant concentrations of ammonium acetate and sodium chloride are required at the beginning of the gradient (up to > 5 M) to achieve a proper separation of mAbs and DAR species of ADC. Therefore, ammonium sulfate and sodium acetate seemed to be the most appropriate ones for protein biopharmaceuticals characterization in HIC (1 M of ammonium sulfate was equivalent to ~2–3 M of ammonium acetate), and also provided better peak shapes. At the end, we propose a fast and automated "phase system" (i.e. stationary phase and salt type) optimization procedure for the analytical characterization of protein biopharmaceuticals. Then, the analytical conditions (gradient profile and temperature) were fully optimized by computer assisted retention modeling.

Acknowledgements

The authors acknowledge Marie-Clarie Janin-Bussat (Centre d'Immunologie Pierre Fabre, Saint-Julien en Genevois, France) for helpful discussions on ADC and mAb HIC separations. Elsa Wagner, Laura Morel-Chevillet and Mélissa Excoffier (Centre d'Immunologie Pierre Fabre, Saint-Julien en Genevois, France) are also acknowledged for p*I* calculation and measurements by IEF and cIEF. We also wish to thank Dr. Imre Molnar and Dr. Hans-Jürgen Rieger (Molnár Institute, Berlin, Germany) for the scientific discussions. Marleen van Wingerden (Waters) is also acknowledged for offering the Protein-Pak column. Finally, we acknowledge Prof. Jean-Luc Veuthey (School of Pharmaceutical Sciences, University of Geneva, Switzerland) for scientific discussions and his suggestions, corrections.

Davy Guillarme wishes to thank the Swiss National Science Foundation for support through a fellowship to Szabolcs Fekete (31003A_159494).

References

[1] S. Hjerten, Some general aspects of hydrophobic interaction chromatography, J.Chromatogr. 87 (1973) 325–331.
[2] J.A. Querioz, C.T. Tomaz, J.M.S. Cabral, Hydrophobic interaction chromatography of proteins, J. Biotech. 87 (2001) 143–159.
[3] M. Rodriguez-Aller, D. Guillarme, A. Beck, S. Fekete, Practical method development for the separation of monoclonal antibodies and antibody-drug conjugate species in hydrophobic interaction chromatography, part 1: optimization of the mobile phase, J. Pharm. Biomed. Anal. 118 (2016) 393–403.
[4] G. Rippel, L. Szepesy, Hydrophobic interaction chromatography of proteins on an Alkyl-Superose column, J. Chromatogr. A 664 (1994) 27–32.
[5] L. Szepesy, G. Rippel, Comparison and evaluation of HIC columns of different hydrophobicity, Chromatographia 34 (1992) 391–397.
[6] L. Szepesy, G. Rippel, Effect of the characteristics of the phase system on the retention of proteins in hydrophobic interaction, J. Chromatogr. A 668 (1994) 337–344.
[7] S. Fekete, J.L. Veuthey, D. Guillarme, Modern column technologies for the analytical characterization of biopharmaceuticals in various liquid chromatographic modes, LCGC, Eur, in: K. Sandra, P. Sandra (Eds.), Advances in Biopharmaceutical Analysis, 2015, pp. 8–15.
[8] L.N. Lee, J.M.R. Moore, J. Ouyang, X. Chen, M.D.H. Nguyen, W.J. Galush, Profiling antibody drug conjugate positional isomers: a system-of equations approach, Anal. Chem. 84 (2012) 7479–7486.
[9] F. Debaene, A. Boeuf, E. Wagner-Rousset, O. Colas, D. Ayoub, N. Corvaïa, A. Van Dorsselaer, A. Beck, S. Cianferani, Innovative native MS methodologies for antibody drug conjugate characterization: high resolution native MS and IM-MS for average dar and dar distribution assessment, Anal. Chem. 86 (2014) 10674–10683.
[10] A. Vallaja, C. Horváth, Retention thermodynamics in hydrophobic interaction chromatography, Anal. Chem. 35 (1996) 2964–2981.
[11] J.F. Valliere-Douglass, W.A. McFee, Oscar Salas-Solano, Native intact mass determination of antibodies conjugated with monomethyl auristatin E and F at interchain cysteine residues, Anal. Chem. 84 (2012) 2843–2849.
[12] N.S. Beckley, K.P. Lazzareschi, H.W. Chih, V.K. Sharma, H.L. Flores, Investigation into temperature-induced aggregation of an antibody drug conjugate, Bioconjugate. Chem. 24 (2013) 1674–1683.
[13] L.R. Snyder, M.A. Stadalius, in: Csaba Horváth (Ed.), High-Performance Liquid Chromatography, Advances and Perspectives, vol. 4, Academic Press, New York, 1986, p. 195.
[14] L.R. Snyder, J.J. Kirkland, J.L. Glajch, Practical HPLC Method Development, 2nd ed., John Wiley & Sons Inc., 1997.
[15] G. Rippel, Á. Bede, L. Szepesy, Systematic method development in hydrophobic interaction chromatography I. Characterization of the phase system and modelling retention, J. Chromatogr. A 697 (1995) 17–29.
[16] D. Guillarme, D.T.T. Nguyen, S. Rudaz, J.L. Veuthey, Method transfer for fast liquid chromatography in pharmaceutical analysis: application to short columns packed with small particle part II: gradient experiments, Eur. J. Pharm. Biomed 68 (2008) 430–440.
[17] J.C. Ford, J. Ko, Comparison of methods for extracting linear solvent strength gradient parameters from gradient chromatographic data, J. Chromatogr. A 727 (1996) 1–11.
[18] K. Valkó, P. Slégel, New chromatographic hydrophobicity index ($\acute{o}_0$) based on the slope and the intercept of the log ké versus organic phase concentration plot, J. Chromatogr. 631 (1993) 49–61.
[19] B. Wiggins, L.L. Shin, H. Yamaguchi, G. Ratnaswamy, Characterization of cysteine-linked conjugation profiles of immunoglobin G1 and immunoglobin G2 antibody-drug-conjugates, J. Pharm. Sci. 104 (2015) 1362–1372.
[20] M. Haverick, S. Mengisen, M. Shameem, A. Ambrogelly, Separation of mAbs molecular variants by analytical hydrophobic interaction chromatography HPLC: overview and applications, mAbs 6 (2014) 852–858.
[21] A. Beck, J.F. Haeuw, T. Wurch, L. Goetsch, C. Bailly, N. Corvaia, The next generation of antibody-drug conjugates comes of age, Discov. Med. 10 (2010) 329–339.
[22] M.C.J. Bussat, M. Dillenbourg, N. Corvaia, A. Beck, C.K. Hamour, Characterization of antibody drug conjugate positional isomers at cysteine residues by peptide mapping LC–MS analysis, J. Chromaotgr. B 981-982 (2015) 9–13.
[23] J.W. Dolan, L.R. Snyder, N.M. Djordjevic, D.W. Hill, D.L. Saunders, L. Van Heukelem, T.J. Waeghe, Simultaneous variation of temperature and gradient steepness for reversed-phase high-performance liquid chromatography method development: I. Application to 14 different samples using computer simulation, J. Chromatogr. A 803 (1998) 1–31.
[24] L.R. Snyder, J.J. Kirkland, J.L. Glajch, Practical HPLC Method Development, 2nd ed., John Wiley & Sons Inc., 1997.
[25] S. Fekete, S. Rudaz, J. Fekete, D. Guillarme, Analysis of recombinant monoclonal antibodies by RPLC: toward a generic method development approach, J. Pharm. Biomed. Anal. 70 (2012) 158–168.

[26] S. Fekete, A. Beck, J. Fekete, D. Guillarme, Method development for the separation of monoclonal antibody charge variants in cation exchange chromatography, part I: salt gradient approach, J. Pharm. Biomed. Anal. 102 (2015) 33–44.
[27] S. Fekete, A. Beck, J. Fekete, D. Guillarme, Method development for the separation of monoclonal antibody charge variants in cation exchange chromatography, part II: pH gradient approach, J. Pharm. Biomed. Anal. 102 (2015) 282–289.
[28] R. Kormány, I. Molnár, J. Fekete, D. Guillarme, S. Fekete, Robust UHPLC separation method development for multi-API product containing amlodipine and bisoprolol: the impact of column selection, Chromatographia 77 (2014) 1119–1127.
[29] J.R. Montano, C.O. Bolsico, M.J.R. Angel, M.C.G.A. Coque, Implementation of gradients of organic solvent in micellar liquid chromatography using DryLab®: separation of basic compounds in urine samples, J. Chromatogr. A 1344 (2014) 31–41.
[30] I. Molnar, Computerized design of separation strategies by reversed-phase liquid chromatography: development of DryLab software, J. Chromatogr. A 965 (2002) 175–194.